

Automated Evaluation System for Human Pupillary Behavior

Cleyton Rafael Gomes Silva^a, Cristhiane Gonçalves^b, Eduardo N. R. Camilo^c, Fabio Boaretti dos Santos^c, Joyce Siqueira^a, Eduardo Simões de Albuquerque^a, Fabrizzio Alphonsus Alves de Melo Nunes Soares^a, Leandro Luís Galdino de Oliveira^a, Ronaldo Martins da Costa^a

^aInstitute of Informatics, Federal University of Goiás, Goiania, Goiás, Brazil,

^bInstitute of Physics, Federal University of Goiás, Goiania, Goiás, Brazil

^cGoiás Eye Bank Hospital, Goiania, Goiás, Brazil

Abstract

Analyzing human pupillary behavior is a non-invasive method for evaluating neurological activity. This method contributes to the medical field because changes in pupillary behavior can be correlated with several health conditions such as Parkinson, Alzheimer, autism and diabetes. Analyzing human pupillary behavior is simple and low-cost, and may be used as a complementary diagnosis. Therefore, this work aims to develop an automated system to evaluate human pupillary behavior. The solution consists of a portable recording device, a pupillometer; integrated with a recording and evaluation software based on computer vision. The system is able to stimulate, record, measure and extract relevant features of human pupillary behavior. The results show that the proposed system is fast and accurate, and can be used as an assessment tool for real and extensive clinical practice and research.

Keywords:

Pupil; Computers

Introduction

Human pupillary behavior has been an increasingly important subject in scientific research, showing promising contributions to biometrics [1] and mostly to the medical field [2,3]. Controlled by the autonomic nervous system to provide more accurate vision and ensure retinal integrity [4], this behavior is considered a non-invasive and alternative method to assess neurological activity [3]. Abnormal pupillary behavior can indicate diseases and neurological disorders such as Parkinson [5], Alzheimer [6], autism [7] and diabetes [8].

This pupillary behavior is based on two reflexes, contraction and dilation, or miosis and mydriasis; both are involuntary reactions and are triggered to manage the amount of light entering the eyes [4]. Pupil size management depends on the illuminance level to which the eyes are exposed. Pupil size is inversely proportional to illuminance level. Contraction occurs as the illuminance level increases [9] while dilation occurs whenever illuminance level decreases [10].

As an important biosignal and potential indicator of health states, pupillary behavior is often evaluated by measuring pupil diameter over time under light stimuli, a process known as Pupillometry [11]. This method usually depends on modern technology composed by devices equipped with infrared cameras, which is able to record images even in low light conditions. Such devices, combined with software solutions

based on computer vision, are responsible for image acquisition, processing and feature extraction, essential steps for research involving monitoring pupillary behavior.

In this scenario, automated pupillometry solutions can provide effective technology to extract reliable data for patient medical evaluation. Previous studies have shown advances, presenting recording devices in many formats, from robust and large equipment [12] to solutions made with regular materials, as a common eyeglass frame [13]. However, the proposals are not always viable or portable devices with fully integrated systems for real and extensive clinical and research practice.

Therefore, this work aims to develop a portable and comfortable recording device, a pupillometer; with an automated and integrated evaluation system based on computer vision to perform pupillometry procedures. These two components combined form an Automated Pupillometry System (APS), capable of stimulating, recording, measuring and extracting relevant human pupillary behavior features. Results demonstrate the system as a useful and efficient solution and tool for medical and research investigations.

Methods

The method is presented accordingly in the Automated Pupillometry System (APS) stages (Figure 1).

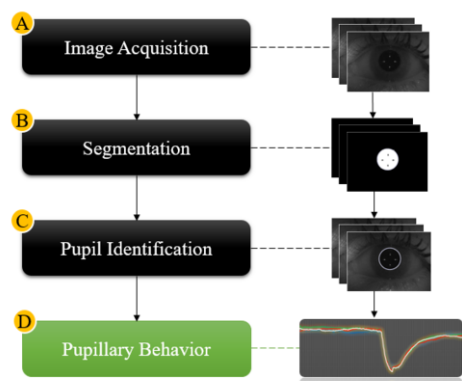


Figure 1— Stages of the Automated Pupillometry System (APS): (A) Image Acquisition; (B) Segmentation; (C) Object Identification and (D) Pupillary Behavior.

The first subsection, Image Acquisition, describes the pupilometer resources and operation, recording function of the software, participants description and the pupillometry protocol applied. The second subsection, Segmentation and Pupil Identification, presents the image processing to highlight the pupil in images and explains the measurement of pupillary diameter. The third subsection, Pupillary Behavior, shows the feature extraction.

Imagem Acquisition

Pupillometer

The recording device (Figure 2) was built by adapting a virtual reality glasses frame. Two infrared cameras were attached to two acrylic plates, and then on a printed circuit board with an eyeglass shape. The cameras are Point Grey's mono firefly, FMVU-03MTM-CS model, CMOS sensor (global shutter) and have a USB 2.0 interface. The circuit board was configured to control five RGB LEDs and four infrared LEDs on each side. Infrared LEDs provide illumination for a low light condition whereas RGB LEDs are used for stimuli.



Figure 2– (A) Pupillometer Off; (B) Pupillometer On.

On each side, Infrared LEDs were arranged in a rhombus format, Figure 2 (B), from five RGB LEDs; four were arranged in a square form and the last one fixed below the acrylic plate. These plates have a circle drawn and become visible by turning the lower LEDs on. Used to guide the gaze, the orientation circle's luminosity is adjusted so the patient can locate them without triggering pupillary reflexes. During the procedures, to avoid distraction, this circle is lit only in the non-stimulated side.

Recording Interface

The developed software was built in Matlab® R2016b platform, using the following toolboxes: image acquisition, image processing, parallel computing and Matlab GUI (graphical user interface). The first window is dedicated to the recording procedures (Figure 3) and has six operation modes, separated by a stimulated and a recorded side, as follows:

1. Stimulated Eye: Right; Recorded Eye: Right.
2. Stimulated Eye: Left; Recorded Eye: Right.
3. Stimulated Eye: Right; Recorded Eye: Both.
4. Stimulated Eye: Left; Recorded Eye: Left.
5. Stimulated Eye: Right; Recorded Eye: Left.
6. Stimulated Eye: Left; Recorded Eye: Both.

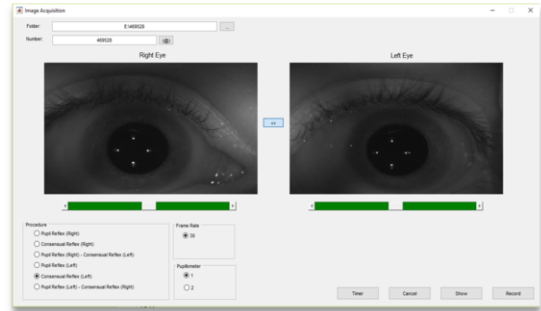


Figure 3– APS Record Window.

In addition to the direct reflection, which is the result of the behavior of the stimulated eye, options: 2, 3, 5 and 6 were created to evaluate consensual reflex, because both pupillary reflexes are expected to be symmetrical, regardless of which side is illuminated [4,14]. This particularity has a medical value as asymmetries are an indicator of optic nerve and retinal diseases [14], as well as brain trauma [4].

In this part of the system, fields and buttons allow users to: define the destination folder and the patient's ID; display the camera feeds; initiate the timer for dark adaptation; and start or abort recording procedures. The videos are recorded at 30 fps with 640x480 pixels resolution (Figure 5 (A)) and exported in an uncompressed AVI file with the name formed by the patient's ID plus the letter 'R' or 'L', depending on the recorded side.

Participants

All experimental procedures were reviewed and approved by the Research Ethics Committee in a project submitted to the Brazil platform, under CAAE number: 57179216.8.0000.0033. Forty volunteers were recruited and agreed to participate in this research by signing a free and informed consent term. The research aim and details were explained to all.

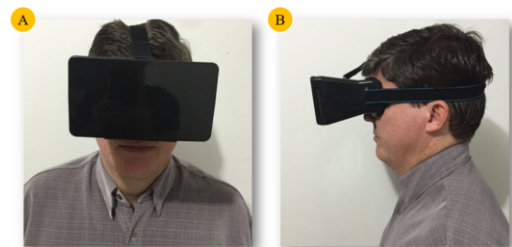


Figure 4– The pupillometer being used by a volunteer: (A) Front View; (B) Side View.

For all cases, the fifth operation mode was selected. As the pupillometer design isolates most of the external illumination, as demonstrated in Figure 4, the infrared LEDs are switched on at the beginning of the software execution (Figure 3) as well as the orientation circle. The volunteers were advised to avoid blinking and to fix the gaze guided by the orientation circle. Then the pupillometry protocol was applied, as follows.

Pupillometry Protocol

The pupillometry protocol (Figure 5) was designed to satisfy three goals: a dark adaptation period of 10 minutes to reach maximum dilation [15], stimuli in colors used for medical [16,17] and biometrics [1] research, and lightless intervals between stimuli to allow the recovery of pupillary size. All these goals were combined in 14:05 minutes.

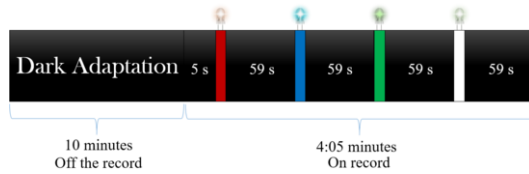


Figure 5– Pupillometry Protocol.

Procedures begin with pupillary adaptation in a room with lights off, <1 lux. After the pupillometer is put in position (Figure 4), the software starts recording the first five seconds to register dilation and continues with a cycle of four stimuli with a 1 second duration each, every 59 seconds, in red-blue-green-white order. All stimuli were set in scotopic condition (100 lux) and the intensities were checked by a TASI-8721 light meter, with $\pm 4\%$ rdg ± 10 dgts ($< 10,000$ lux) of accuracy. Infrared LEDs were adjusted considering the limit for the eyes' exposure [18] to 4:05 minutes of recording procedure.

Segmentation and Pupil Identification

Through segmentation, the pupillary region can be isolated and measured in the images. The end result is a signal of the pupillary diameter as a function of time, representing the patient pupillary behavior during the procedure. This signal gives rise to relevant features used to evaluate the pupil behavior. In this work the segmentation proposal consists of six steps (Figure 6).

Gaussian Filtering

The first step, Figure 6 (A), eliminates noise in images. Noise might cause interference in the subsequent processes. Noise is relatively common in the image acquisition process and to minimize the effects, smoothing techniques can be applied [19]. Thus, at this stage, the images are smoothed using a Gaussian filter with $\sigma = 2$ and window size = 9. These parameters, defined experimentally, allow most of the noise to not be highlighted in the binarization.

Binarization (Weighted Otsu)

Through the binarization, regions in the image can be highlighted in two different colors; black and white. For this division to be made, a threshold representing the intensity that divides such regions needs to be defined. Although the pupil represents a large and connected dark region in the image, finding the ideal threshold is not a trivial task. Position, color of adjacent areas, facial structure, color and intensity of stimuli, and proximity to the camera are examples of situations where image characteristics can change dramatically. In these cases the same threshold does not get a correct separation.

In this scenario it is important to adapt to these changes and to perform binarization using automatic thresholds. In this step, a segmentation similar to that used in [20] is applied, when using the Otsu's method. This method seeks to minimize the sum of the object and background variance. For this, the technique performs iteration for all possible thresholds until it finds one that minimizes the sum of the object and background variances.

This method applied to an image that contains the eye structure tends to separate the sclera region, white region, from the pupil and iris, darker regions. However, in order to restrict the pupillary region of the iris region, a weighting factor of 2.5 is applied. This weighting of the otsu value (WO) is efficient and adaptive, as can be seen in the values and results shown in Figure 6 (B). The factor was defined by means of empirical tests on images with different illuminations, proximities and ocular structures.

Morphological Filtering

During the recording procedure and due to the stimuli and the infrared illumination, videos have moments with different levels of illumination. The main difficulty is the presence of reflexes produced by the cornea. For this reason part of the pupillary region is not captured or is extremely compromised (Figure 6 (A-2)). In order to overcome this problem, morphological operations of opening and closing in conjunction with a flood-fill process to close holes are applied in the image resulting from the binarization (Figure 6 (C)).

Numeric Shape Descriptor

Once the objects are isolated in the previous process, there is the possibility that other objects may be highlighted, such as: remaining noises, occluded pupil, pupil with a large part covered by the eyelid and/or eyelashes, as can be seen in Figure 6 (C- 2), or another large dark region. A numeric shape descriptor is used to recognize the pupil or detect moments in which measurement is not possible, such as blinking occasions.

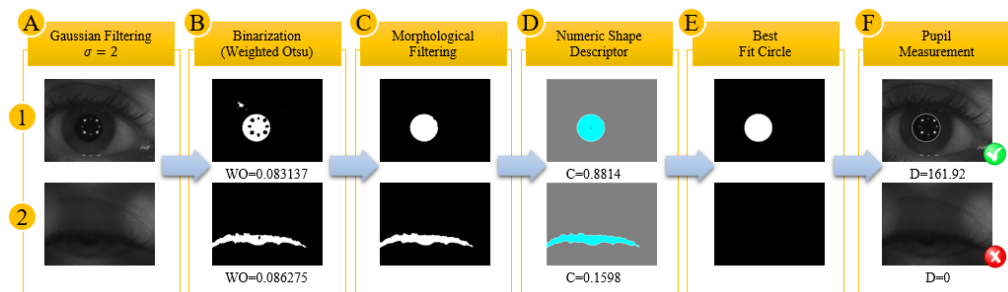


Figure 6– Segmentation: (A) Gaussian Filtering; (B) Binarization (Weighted Otsu); (C) Morphological Filtering; (D) Numeric Shape Descriptor; (E) Best Fit Circle and (F) Pupil Measurement, (1) Normal, (2) Blinking.

To recognize the pupil or detect moments that there is no possibility of measurement, such as blinking moments, a numeric shape descriptor is used.

The descriptor, equation 1, allows the circularity of the objects in the image to be calculated [19]. The value resulting from the calculation approaches 1 as the circularity increases, and the value 1 represents a perfect circle. Considering that the pupil does not represent a perfect circle and that in some moments there will be deformations resulting from reflexes, a threshold of 0.65 was experimentally defined and proved to be effective. This value allows to separate images eligible for measurement from those where there is absence of a sufficient pupillary region, as shown in Figure 6 (D-2).

$$C = \frac{4\pi * Area}{Perimeter^2} \quad (1)$$

Best Fit Circle and Measurement

Images identified with circular objects pass through a last step before they have their diameter measured. To correctly measure the diameter, even in images whose pupil is partially segmented, a circular fitting process (Figure 6 (E)) calculates the circle that best fits the rectangular limits of the object. This procedure allows for a simple and fast operation to find the approximate pupil diameter (Figure 6 (F)). The diameter extracted through this process is a good approximation of the actual diameter even in images with partial pupils. For research that aims to use the iris boundaries, where it is important to isolate the original pupil shape, the method is also efficient. In these cases the fitting step should be ignored.

Pupillary Behavior

Feature Extraction

The points of interest in the data are those closest to the stimuli. For this, the signal is decomposed by the system in four parts, one for each region influenced. Representing five seconds prior and ten subsequent to a second of stimulus, each decomposed signal represents sixteen seconds of observation. Eight features are extracted from each signal. These features are relevant in order to understand changes in human pupillary behavior [11,21]. Such features are given in Figure 7.

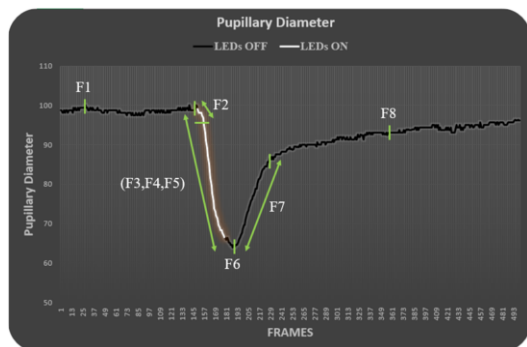


Figure 7– Features: F1- Maximum dilation; F2-Latency; F3- Time to maximum contraction; F4- Relative amplitude; F5- Absolut amplitude; F6- Maximum contraction; F7-Post-Illumination response; F8-6 sec test.

F1. Maximum dilation: maximum diameter registered in the signal, usually found in the period before the start of the stimulation.

F2. Latency: time spent in seconds between the start of the stimulus and the beginning of the process of contraction, thus considered as a 10% change in diameter.

F3. Time to maximum contraction: time spent in seconds between the start of the stimulus and the maximum contraction registered.

F4. Relative amplitude: percentage value of the difference between the largest and smallest diameter.

F5. Absolute amplitude: absolute value of the difference between the pupillary diameter before the stimulus and the value of maximum contraction.

F6. Maximum contraction: smaller diameter contraction registered, usually found during stimulation.

F7. Post-Illumination response: time in seconds the pupillary diameter takes after the stimulus to achieve 85% of the previous value.

F8. 6 sec test: diameter registered 6 seconds after the end of the stimulus.

Results and Discussion

In this research, the experiment was accomplished with 40 volunteers. In all cases both eyes were recorded with the right side receiving stimuli. As each video was recorded at 30 frames per second, they are composed of 7.350 frames each. The procedure was able to extract the pupil behavior using the diameter and calculate the features successfully in all cases. A total of 588.000 frames were processed by the system. At the end of each processing a screen displays the results, as shown in Figure 8. All data are stored automatically in an Excel file, with the diameter values in pixels and percentage scales. The file also contains a comparison between the left and right side.

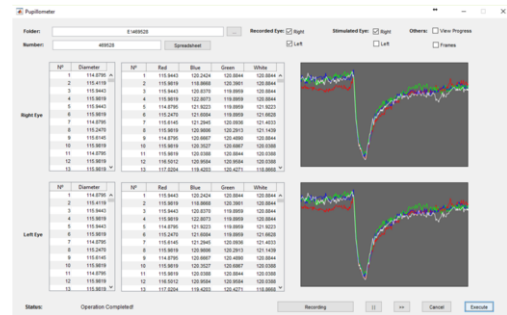


Figure 8– APS Main Window.

In order to measure the performance and effectiveness of the segmentation process, the images from each participant were separated into five categories, one for the moment without stimulation and one for each color used: red, blue, green and white. This is justified by the fact that each color of stimulus changes the features of the image differently. After this separation, two images for each period and participant were randomly selected, totaling 400 images.

Through segmentation of the selected images, the average speed processing was 347.84 milliseconds. For testing, a computer with intel core i5 processor and 4 GB of RAM was used. For the calculation of accuracy, the number of correct segmentations was divided by the total number of images. By means of this calculation, the percentage of accuracy of the approach reached the value of 97.25%.

It is worth mentioning that the images on which the method was not successful were those whose pupil was partially covered by eyelashes or eyelids. Images on which the pupil was totally or practically covered were eliminated and replaced by a new image of the same category. It is important to emphasize that the numeric shape descriptor used allowed 100% of these cases of pupillary occlusion to be automatically excluded.

Conclusion

This study proposes an Automated Pupillometry System (APS). The segmentation process is essential for this approach and is fast and effective, reaching a level of accuracy of 97.25 %. This factor allowed the system to be able to extract 8 important features of the human pupillary behavior for each type of stimulus, totalizing 32 features. All the processes from the acquisition, to the generation of the data in the file were made in automated form; fulfilling the main goal of this work.

Blinking is one of the main problems in pupil segmentation and the main cause of noise in data. The usage of a shape descriptor is able to remove it in its totality. Therefore, the system represents an efficient pupillometry solution for extensive practices in medical and research investigations. In future work, the objective is to implement functions to allow the pupillometry protocol to be customized, considering the time, color and interval between stimuli. This will make procedures more flexible for even wider use.

Acknowledgements

This research is financially supported by Coordination for the Improvement of High Level Personnel - CAPES.

References

- [1] R.M. da Costa and A. Gonzaga, Dynamic Features for Iris Recognition, *IEEE Transactions on Systems, Man, and Cybernetics, Part B (Cybernetics)* **42** (2012), 1072-1082.
- [2] K. Yamaji, Y. Hiratai, and S. Usui, The pupil as a possible monitor of the autonomic nervous system, in: *Proceedings of the 19th Annual International Conference of the IEEE Engineering in Medicine and Biology Society: 'Magnificent Milestones and Emerging Opportunities in Medical Engineering'* (Cat. No.97CH36136), IEEE, 1997.
- [3] Y. Altay, M.M. Altay, G. Demirok, O. Balta, and H. Bolu, Measurements of Pupillary Diameter and Wavefront Aberrations in Pregnant Women, *Scientifica* **2016** (2016), 1-5.
- [4] D. Purves, *Neuroscience*, Sinauer Associates, Publishers, Sunderland, Mass., 2004.
- [5] C.-A. Wang, H. McInnis, D.C. Brien, G. Pari, and D.P. Munoz, Disruption of pupil size modulation correlates with voluntary motor preparation deficits in Parkinson's disease, *Neuropsychologia* **80** (2016), 176-184.
- [6] F. Fotiou, K.N. Fountoulakis, M. Tsolaki, A. Goulas, and A. Palikaras, Changes in pupil reaction to light in Alzheimer's disease patients: a preliminary report, *International Journal of Psychophysiology* **37** (2000), 111-120.
- [7] H.J. Nuske, G. Vivanti, K. Hudry, and C. Dissanayake, Pupillometry reveals reduced unconscious emotional reactivity in autism, *Biological Psychology* **101** (2014), 24-35.
- [8] K. Hayashi and H. Hayashi, Pupil size before and after phacoemulsification in nondiabetic and diabetic patients, *Journal of Cataract and Refractive Surgery* **30** (2004), 2543-2550.
- [9] T.M. Gable, A.L. Kun, B.N. Walker, and R.J. Winton, Comparing heart rate and pupil size as objective measures of workload in the driving context, in: *Adjunct Proceedings of the 7th International Conference on Automotive User Interfaces and Interactive Vehicular Applications - AutomotiveUI '15*, ACM Press, 2015.
- [10] C.-A. Wang and D.P. Munoz, A circuit for pupil orienting responses: implications for cognitive modulation of pupil size, *Current Opinion in Neurobiology* **33** (2015), 134-140.
- [11] H. M. Pinheiro, E. Nery, R. Camilo, M. Oftalmologista, and R. Martins Da Costa, Metodologia e Dispositivo Portátil para Avaliação do Re-

- flexo Pupilar, in: *21st Americas Conference on Information Systems, AMCIS 2015*, Association for Information Systems, Puerto Rico, 2015.
- [12] W. Nowak, A. Zarowska, E. Szul-Pietrzak, and M. Misiuk-Hojto, System and measurement method for binocular pupillometry to study pupil size variability, *Biomed Eng Online* **13** (2014), 69.
- [13] Y.-C. Tsai, Y.-J. Yan, M.-L. Ko, T.-W. Huang, J.-C. Chiou, and M. Ou-Yang, Design of synchronizing pupillometer for observing nerve conduction by pupillary responses, in: *2016 IEEE International Instrumentation and Measurement Technology Conference Proceedings*, IEEE, 2016.
- [14] O. Bergamin, M.B. Zimmerman, and R.H. Kardon, Pupil light reflex in normal and diseased eyes, *Ophthalmology* **110** (2003), 106-114.
- [15] L.A.R. Gabriel, N.S. Peachey, and J.S. Sunness, Retinal Function Testing and Genetic Disease, in: *Genetic Diseases of the Eye*, Oxford University Press, 2012, pp. 343-355.
- [16] S. Traustason, A.E. Brondsted, B. Sander, and H. Lund-Andersen, Pupillary response to direct and consensual chromatic light stimuli, *Acta Ophthalmologica* **94** (2015), 65-69.
- [17] M. Bernabei, L. Rovati, L. Peretto, and R. Tinarelli, Measurement of the pupil responses induced by RGB flickering stimuli, in: *2015 IEEE International Instrumentation and Measurement Technology Conference (I2MTC) Proceedings*, IEEE, 2015.
- [18] E. Allen, Eye Safety for Proximity Sensing Using Infrared Light-Emitting Diodes Photobiological Effects of Application Note 1737 IEC-62471, *Photobiological* (2012), 1-11.
- [19] J.C. Russ, Image analysis and signal processing in electron microscopy. P. W. Hawkes, W. Owen Saxton, F. Peter Ottensmeyer and Azriel Rosenfeld (Editors). Published by Scanning Microscopy International, 1988, Chicago, IL, USA; ISSN 0892-953X, *X-Ray Spectrometry* **18** (1989), 247-247.
- [20] M. Abdullah, Fast and Accurate Pupil Isolation Based on Morphology and Active Contour, *International Journal of Information and Electronics Engineering* **4** (2014).
- [21] P. Adhikari, A.J. Zele, and B. Feigl, The Post-Illumination Pupil Response (PIPR), *Investigative Ophthalmology & Visual Science* **56** (2015), 3838.

Address for correspondence

Cleyton Rafael Gomes Silva, E-mail: cleytonrafael@inf.ufg.br.